Enhancement of power factor in zinc antimonide thermoelectric thin film doped with titanium

Zhuang-Hao Zheng, Fu Li, Jing-Ting Luo, Guang-Xing Liang, Hong-Li Ma, Xianghua Zhang, Ping Fan

Enhancement of power factor in zinc antimonide thermoelectric thin film doped with titanium

Zhuang-hao Zheng [a, b], Fu Li [a, *], Jing-ting Luo [a], Guang-xing Liang [a, b], Hong-li Ma [b], Xiang-hua Zhang [b], Ping Fan [a, *]

[a] *Institute of Thin Film Physics and Applications, Shenzhen Key Laboratory of Advanced Thin Films and Applications, College of Physics and Energy, Shenzhen University 518060, China*

[b] *Laboratory of Glasses and Ceramics, Institute of Chemical Science UMR CNRS 6226, University of Rennes 1, Rennes 35042, France*

[*] Corresponding author. E-mail: lifu@szu.edu.cn and fanping308@126.com

Abstract

Titanium doped zinc antimonide thin films were prepared on flexible substrates by multi-step co-sputtering method, which can assure that the Ti is homogeneous distribution in the thin film. The influence of Ti content on the microstructure and thermoelectric properties of the ZnSb based thin films was systematically investigated. The high-resolution transmission electron microscopy and X-ray diffraction exhibit that the sample has nano-sized crystallite, which will lead to better thermoelectric properties. The electrical conductivity of the Ti-doped ZnSb thin films is stable at the temperature ranging from room-temperature to 200 °C and then it has a significant increase when the temperature continues increasing. As expected, the power factor of the thin film has almost 80 % enhancement after Ti doped.

Keyword: Sputtering, Thin films

1. Introduction

Recently, thermoelectric material based thin films and their generators have applied a huge potential application in miniaturization sensors, micropower source and other thermoelectric application for micro-devices [1-5]. The performance of thermoelectric materials is determined by the dimensionless figure of merit (ZT) which is defined as $S^2T\sigma/\kappa$, where S is the Seebeck coefficient, T is the absolute temperature, σ is the electrical conductivity and κ is the thermal conductivity [6]. ZnSb binary thin film is one of the promising P-type thermoelectric materials for low cost thermoelectric application. Further improvements in its properties are imperative. Metal doping is a function way and has been widely studied to optimize the thermoelectric

performance of materials [9-12]. Titanium is a typical metal with high melting point and has been reported that the properties of materials, such as electrical conductivity and thermostability, can be enhanced after its doping [13]. Additionally, some researches shown that the doped thin films fabricated by multi-layer method always have high quality due to its phase evolution and sufficient diffusion of elements [14-17].

In this work, we report the thermoelectric properties of the Ti-doped ZnSb thin film. The multi-step co-sputtering process was used to assure the Ti can be homogeneous distribution in the thin film. In addition, the flexible substrate was used and it benefits for further low-cost and large-scale industrial production.

2. Experimental

High purity (4N) Ti target and ZnSb alloy target with the atomic ration of 4 (Zn):3 (Sb) were used. The kapton type polyimide with the thickness of 0.15 mm was used as the flexible substrate. The chamber was pumped to a base pressure of 6.0×10^{-4} Pa and the working pressure was kept at 0.4 Pa with Ar as the working gas. The sputtering power of ZnSb was kept at 50 W and the deposition time was fixed with 15 min. Figure 1 displays the detail process of fabricating multi-layer specimen. Firstly, the ZnSb was deposited onto the flexible substrate, and the Ti with a very low deposition rate about 0.05 Å was co-sputtered when the ZnSb deposition time was 2 min, 4 min, 6 min, 8 min, 10 min and 12 min, respectively. As Figure 1 shows that the ZnSb thin film within six Ti/ZnSb layer between each ZnSb layer was obtained, and then they were annealed at Ar atmosphere for 1h with the temperature of 598 K.

The structure of the thin films was studied by X-ray diffraction (XRD) technique. The surface morphology of the thin films was obtained by scanning electron microscopy (SEM) and the component analysis was performed by energy dispersive spectroscopy (EDS). Transmission electron microscopy (TEM) has been studied. The carrier concentration and Hall mobility were measured by Van der Pauw Hall measurements at room temperature. The electrical conductivity of the thin films were measured by the four-probe technique. The thin films with two Cu electrodes were performed for the Seebeck coefficient by the measurement system with the

temperature gradient method (ΔK=15K) under air atmosphere.

3. Results and discussion

The Ti content of the thin films is shown in Table 1. It can be seen that the range of the Ti content is 1.7 % ~8 .7 % and the corresponding samples are named as S1, S2, S3, S4 and S5, respectively.

X-ray diffraction patterns of the thin films are shown in Figure 2 (a) and the characteristic pattern of ZnSb (PDF#37-1008) is provided as the comparison. Three main diffraction peaks located at ~26 °, ~28 °, and ~33 ° from Ti-doped ZnSb thin film are defined as the ZnSb (231) (112) and (211) planes, which indicates that ZnSb phase dominates the structure of the sample. There are a few impurity peaks around the angle of ~40 ° and we deduce that those peaks might be the Ti-Sb binary related phase. The crystallite size was calculated by the Debye-Sherrer equation

$$D = \frac{k\lambda}{\beta_{2\theta}\cos\theta}$$

where D is the crystallite size, λ is the wavelength, $\beta_{2\theta}$ is full width half maximum (FWHM) and θ is the angle [19]. Figure 2 (b) shows the calculation result of peak related to (231) plane and (112) plane, and it can be gained that the crystallite size is almost invariable with the size of ~25 nm for (231) and ~ 17 nm for (112). In our early report, the crystallite size of the un-doped ZnSb thin film is 20 nm for (231) [18], suggesting that the grain size expands after Ti doped. The dislocation density is estimated using the relation [19]

$$\rho = \frac{15\varepsilon}{\lambda D}$$

where ε is microstrain which defines as equation [19]

$$\varepsilon = \frac{\left(\beta_{2\theta}\cos\theta\right)}{4}$$

It can be calculated that the largest ρ is the 5.7×10^{-15} cm^{-2} of sample S4 which is lower than the pure ZnSb thin film [18]. In fact, the thin films with lower dislocation density will lead to better mechanical property and electrical property.

The surface topography of the un-doped sample and sample S2 is shown in Figure 3. SEM result indicates that some grains can be observed from the pure ZnSb thin film, but the grains are sparse and irregular which might identify as the clusters rather than grains. After Ti doped, the grains are distinctly observed and distributed evenly, together with the nano-particles structure that the average grain size is less than 50 nm. The HRTEM analyses of S2 affirmatives that the thin film is polycrystalline and numerous grain boundaries can be found in the polycrystalline ZnSb thin film. The grain size is about ~ 13 nm which is coincident with calculation result from XRD, indicating that the thin film has nano-sizes crystallite. Generally, the well-crystallization leads to a better electrical transport and nano-strucutre causes the enhancement of Seebeck coefficient.

Figure 4 (a) shows the carrier concentration n and Hall mobility μ of the Ti doped thin films. The n of S1 is 9.6×10^{19} cm^{-3} and increases to a maximum value of 2.2×10^{20} cm^{-3} of S3, but then it decreases when the Ti content continues increasing. The reduced n of S4 and S5 with the Ti content > 5% is partially due to the recombination of some electrons and holes when Ti^{4+} enter into the lattice according to the defect chemistry, since it created redundant carriers that the intrinsic charge carriers of un-doped ZnSb are holes. The μ has the similar change with respect to the n, and the S3 has a minimum value and S5 has maximum value. Whatever, all the Ti-doped thin films have the large μ which benefits the thermoelectric performance compared with thin film's prepared by other methods [20-22].

The temperature dependents of electrical conductivity σ is shown in Figure 4 (b), it reveals that the room-temperature σ of S1 to S5 samples is ranging of $4.5 \times 10^4 \sim 7.0 \times 10^4$ Sm^{-1}, where the S1 has the maximum value and S2 has the minimum value. The σ of all the specimens shows the increasing trend with the increasing temperature, indicating characteristic semiconductor conduction behavior. Especially, the σ is stabilization and it slightly increases in the temperature interval of 25°C ~ 200 °C, suggesting that the Ti doped thin films have stable thermal performance. Meanwhile, it obviously increases when the temperature rises > 200 °C. Therefore, the stable thermal performance and great electric conduction can owe to the lower dislocation

density after Ti doped that leads to the good mechanical property and lower defects which can reduce the interface scattering of electrons, resulting in the larger σ.

For the thermally activated band conduction in a semiconductor film, the dependence of the conductivity on the temperature T is

$\sigma=\sigma_0 \exp(-E_a/kT)$

where σ_0 is a constant, k is the Boltzman's constant and E_a is the activation energy [23]. The ln (σ) versus 1/T plot inserts in Figure 4 (b) and the calculated activation energy of all the thin films are higher than ~19.8 meV at room-temperature and ~570 meV at high temperature. The value of the activation energy at high temperature is higher than the thin films prepared by other methods [12, 20], indicating lower reaction between the atomics which lead to the more stable electric conduction state.

Figure 4 (c) shows the Seebeck coefficient S of the thin films as a function of Ti content. S1 has a minimum S of 105 μVK^{-1} and it increases to 146 μVK^{-1} of S2. Though the S of S3, S4 and S5 has slightly decreased with the increased Ti content, their values are similar about 135 μVK^{-1}. The S of all the samples increases with the increasing temperature, and the S2 with the Ti content of 2.4 % has the maximum value of 229 μVK^{-1} at 250 °C. However, the S of the Ti doped samples is a little smaller than the un-doped sample [18], which might due to the weak scattering by Ti element which shows a light atomic mass. The power factor ($PF=S^2\sigma$) calculated from the measured σ and S is plotted in Figure 4 (d). The PF of S1 is 0.77 $mWm^{-1}K^{-2}$ and it increases with the increasing of Ti content due to the enhancement of both S and σ at room temperature, indicating that the Ti doping can mediate the conflict of the S and σ, leading the improvement of its thermoelectric properties. In addition, the PF of all the Ti doped thin film is larger than the un-doped thin films and sample S2 has the maximum PF of 3.59 $mWm^{-1}K^{-2}$ at 250 °C which is almost 80 % larger than the un-depoed sample.

4. Conclusion

A series of Ti-doped ZnSb thin films were deposited by multi-step co-sputtering method with various Ti content. The Ti doped thin films with primary ZnSb phase and nano-structure can be

obtained. The electrical conductivity of the Ti-doped samples increases rapidly when the temperature is over 200 °C due to the lower dislocation density and defects. The sample with the Ti content of 2.4 % has the maximum PF of 3.59 $mWm^{-1}K^{-2}$ at 250 °C, which is much higher than the PF value of the un-doped sample. Hence, the Ti doped can optimize the thermoelectric property of the ZnSb thin film.

Acknowledgement

This work is supported by National Natural Science Foundation of China (No. 11604212), Key platform and research projects, Education and Research of Guangdong Province (2015KQNCX139), Basical Research Program of Shenzhen (JCYJ20160307113206388).

References

[1] J.P. Heremans, V. Jovovic, E.S. Toberer, A. Saramat, K. Kurosaki, A. Charoenphakdee, S. Yamanaka, G.J. Snyder, Science 321 (2008) 554-557.

[2] R. Venkatasubramanian, E. Siivola, T. Colpitts, B. O'Quinn, Nature 413 (2001) 597-602.

[3] P. Fan, Z.H. Zheng, Z.K. Cai, T.B. Chen, P.J. Liu, X.M. Cai, D.P. Zhang, G.X. Liang, J.T. Luo, Appl. Phys. Lett. 102 (2013) 033904 1-3.

[4] M. Tan, Y. Deng, Y. Hao, Energy, 70 (2014) 143-148.

[5] P. Fan, Z.H. Zheng, Y.Z. Li, Q.Y. Lin, J.T. Luo, G.X. Liang, X.M. Cai, D.P. Zhang, F. Ye, Appl, Phys, Lett. 106 (2015) 073901 1-4.

[6] D.M. Rowe, CRC handbook of thermoelectrics, CRC press, 1995.

[7] M. Liu, X.Y. Qin, C.S. Liu, L. Pan, H.X. Xin, Phys. Rev. B 81 (2010) 245215 1-10.

[8] Y. Sun, M. Christensen, M. Johnsen, N.V. Nong, Y. Ma, M. Sillassen, E. Zhang, A.E. Palmqvist, J. Bøttiger, B.B. Iversen, Adv. Mater. 24 **(**2012) 1693-1696.

[9] M. Tsutsui, L.T. Zhang, K. Ito, M. Yamaguchi, Intermetallics 12 (2004) 809-813.

[10] K. Valset, X. Song, T. G. Finstad, J. Appl. Phys. 117 (2015) 045709 1-5.

[11] D. Li, H.H. Hng, J. Ma, X.Y. Qin, J. Mater. Res. 24 (2009) 430-435.

[12] A.P. Litvinchuk, J. Nylén, B. Lorenz, A.M. Guloy, U. Häussermann, J. Appl. Phys. 103 (2008) 123524 1-6.

[13] D. Li, X. Y. Qin, J. Appl. Phys. 100 (2006) 023713 1-5.

[14] M.D. Hornbostel, E.J. Hyer, J. Thiel, D.C. Johnson, J. Am. Chem. Soc. 119 (1997) 2665-2668.

[15] B. Mercey, P.A. Salvador, W.Prellier, T.D. Doan, J. Wolfman, M. Hervieu, J. Mater. Chem. 9 (1999) 233-242.

[16] M. Bala, C. Pannu, S. Gupta, T.S. Tripathi, S.K. Tripathi, K. Asokan, D.K. Avasthi, Phys. Chem. Chem. Phys. 17 (2015) 24427-24437.

[17] Z.H. Zheng, P. Fan, Y. Zhang, J.T. Luo, Y. Huang, G.X. Liang, J. Alloys Compd. 639 (2015) 74-78.

[18] P. Fan, W. F. Fan, Z.H. Zheng, Y. Zhang, J.T. Luo, J. Mater. Sci. Mater. Electron, 25 (2014) 5060-5065.

[19] R. Sathyamoorthy, J. Dheepa, J. Phys. Chem. Solid 68 (2007) 111-117.

[20] Z.H. Zheng, P. Fan, J.T. Luo, P.J. Liu, X.M. Cai, G.X. Liang, D.P. Zhang, Intermetallics 64 (2015) 18-22.

[21] A. Bellucci, M. Mastellone, M. Girolami, S. Orlando, L. Medici, A. Mezzi, S. Kaciulis, R. Polini, D.M. Trucchi, Appl. Surf. Sci. 418 (2017) 589-593.

[22] L.T. Zhang, M. Tsutsui. M. Yamaguchi, Thin solid films 443 (2013) 84-90.

[23] K. Niedziolka, R. Pothin, F. Rouessac, R.M Ayral, P, Jund, J. Phys.: Condens. Matter 26 (2014) 365401 1-11.

Figure Captions

Figure 1 Detail process for preparing sample.

Figure 2 (a) XRD patterns of the samples, (b) the crystallite size as function of Ti content

Figure 3 (a) SEM image of the un-doped sample, (b) SEM image of the S2, (c) HRTEM image of S2

Figure 4 (a) the room temperature carrier concentration n and Hall mobility μ for the Ti doped samples, (b) the temperature dependence of electrical conductivity σ, (c) the Seebeck coefficient as the function of the temperature, and (d) PF value as the function of the temperature

Table 1 Ti content of the thin films

Sample	S1	S2	S3	S4	S5
Ti co-sputtering time (min)	1	2	4	10	15
Ti content (at. %)	1.7	2.4	3.3	5.1	8.7

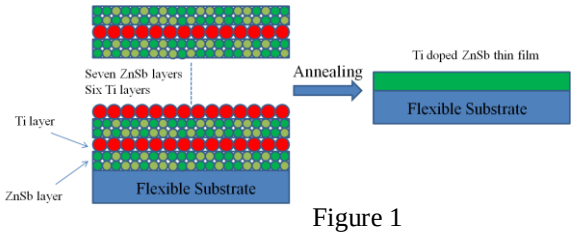

Figure 1

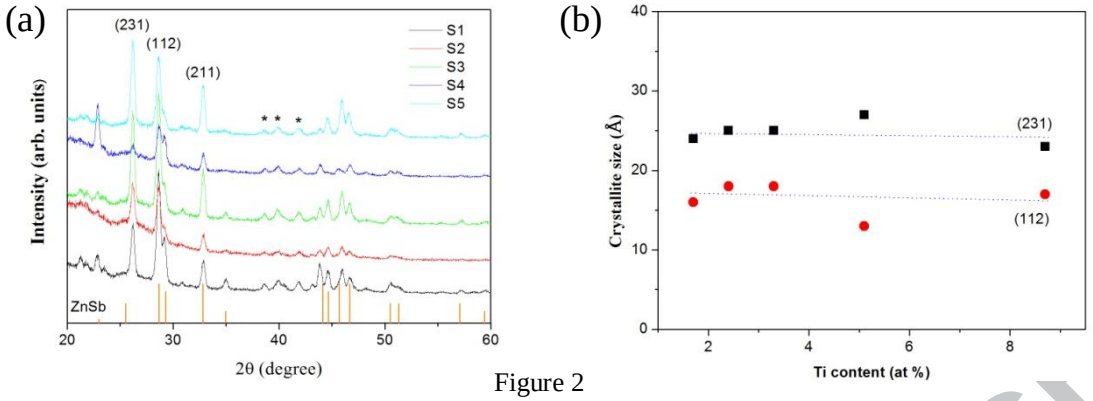

Figure 2

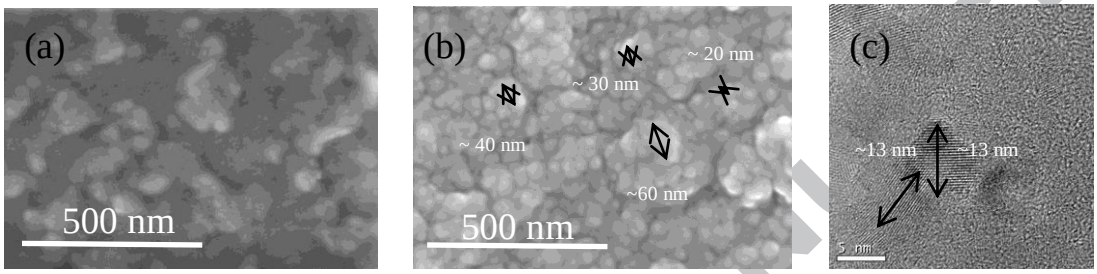

Figure 3 (a) SEM image of the un-doped sample, (b) SEM image of the S2, (c) HRTEM image of S2

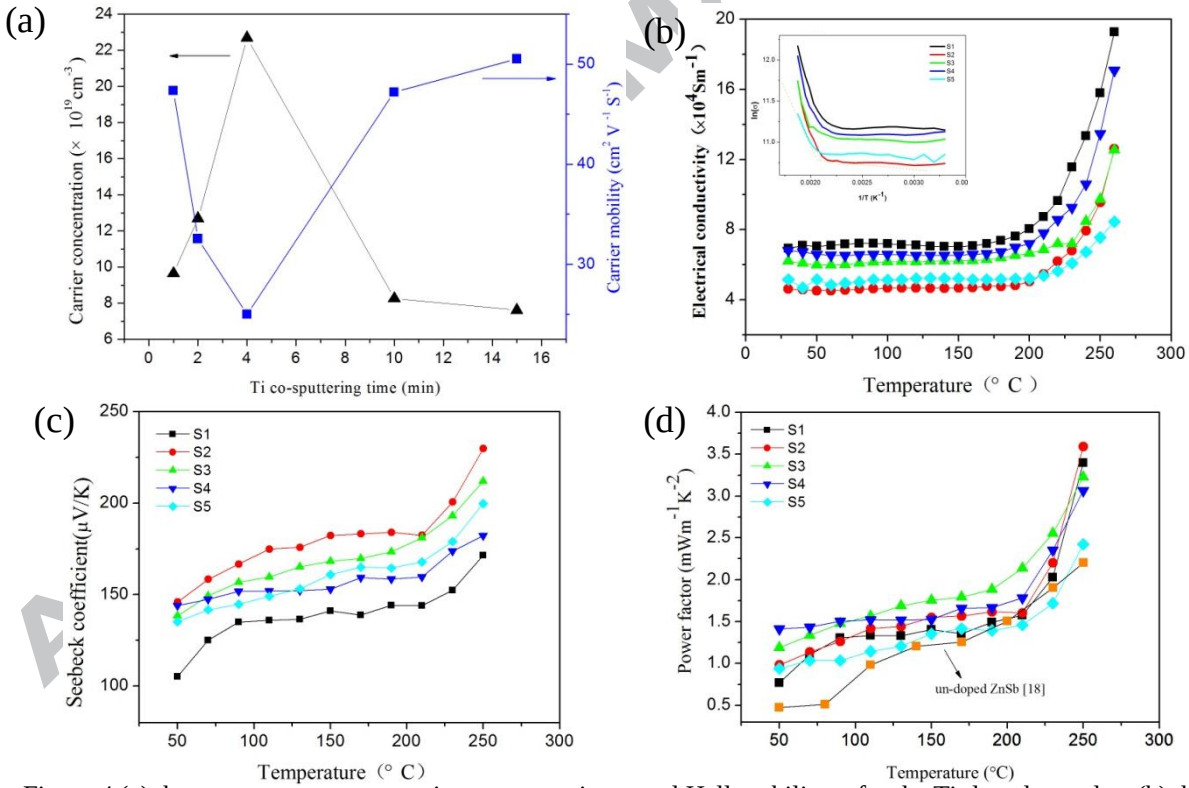

Figure 4 (a) the room temperature carrier concentration n and Hall mobility μ for the Ti-doped samples, (b) the temperature dependence of electrical conductivity σ, (c) the Seebeck coefficient as the function of the temperature, and (d) PF value as the function of the temperature

Highlights

1. Ti doped ZnSb thin films were prepared by multi-step co-sputtering method.

2. The films demonstrate well-crystallized and nano-sized structure.

3. Ti doped can improve thermoelectric properties with both increasing of S and σ.

4. The power factor of the thin film has almost 80 % enhancement after Ti doped.